



## Malaysian Journal on Composites Science and Manufacturing

Journal homepage:  
<https://karyailham.com.my/index.php/mjcs/m/index>  
ISSN: 2716-6945



# Development and Tribological characterisation of Friction Stir Welded Joints of dissimilar metals

Kapil Dev<sup>1</sup>, Hari Om<sup>1,\*</sup>, Tilak Raj<sup>1</sup>

<sup>1</sup> Mechanical Engineering Department, J.C. Bose University of Science and Technology, YMCA, Faridabad, 121006, India

### ARTICLE INFO

#### Article history:

Received 6 January 2026  
Received in revised form 20 February 2026  
Accepted 3 June 2026  
Available online 4 June 2026

#### Keywords:

Friction Stir Welding (FSW); Dissimilar Metal Joints; Intermetallic Compounds; Friction force and Wear rate; Hybrid Taguchi – GRA

### ABSTRACT

In the present work, the development and tribological characterization of friction steel welded FSW joints between dissimilar metals namely Al1060 aluminum and C11000 copper was investigated. Although friction steel welding is widely recognized for producing high quality solid state Joints, Limited studies have focused on the tribological behavior of dissimilar Al-Cu welds. D2 steel tools was employed for welding and nine experiment runs were designed using a L9 Taguchi Orthogonal Array to evaluate the influence of shoulder diameter, rotation, speed and welding speed on the friction force and wear rate. Tribological performance was accessed using a pin-on-disc wear test while worn surface were examined using scanning electron microscopy (SEM). The results revealed that rotational speed was the most influential parameter contributing 37.05% and 84.52% to the variation in friction force and wear rate respectively. The optimum parameter combination Identified through Gray Relation Analysis consists of a shoulder diameter of 22 mm, rotational speed of 1200 RPM and welding speed of 120 mm/min. Under these conditions, the minimum friction force and wear rate obtained were 1000 Newton and 0.0045 mm<sup>3</sup>/Nm respectively representing reductions of approximately 37.5% and 50% compared with the highest value recorded among the tested parameter combinations. SEM observations revealed abrasive and delamination wear mechanism characterized by subsurface crack initiation, debris formation and progressive material removal. The finding establish a clear relationship between FSW process parameters and the tribological performance of dissimilar Al-Cu joints and provide useful guidelines for optimizing welding conditions to enhance wear resistance and service performance in engineering applications.

## 1. Introduction

Welding is a fabrication process used to join metals and thermoplastics. In solid-state welding, pressure and deformation provide a considerable portion of the bonding, and usually no melting of the workpiece is required, and no filler material is usually needed [1]. Forge welding, cold welding, friction welding, explosive welding, diffusion welding, ultrasonic welding, friction stir welding, and friction stir spot welding are some of its examples. Many emerging applications, such as aerospace, nuclear, power generation, and the petrochemical industries, as well as manufacturing, led to the development of friction stir welding for similar and dissimilar materials as one of the leading joining

\* Corresponding author.

E-mail address: hariomjcbose@gmail.com

processes. FSW is used in various industries, including aerospace [2], automotive [3], robotics [4], etc. Thus, previous literature shows that this process is used in many industries; hence process optimization of FSW could lead to the increase of its usage in new sectors to avoid many of the disadvantages of conventional welding techniques, since FSW is a solid-state joining technique. Most of the research conducted shows that friction stir welding between similar metals or alloys has been the prime focus of various researchers, e.g., joining of aluminum to aluminum or steel to steel or pure aluminum to pure copper, etc. Research studies on dissimilar metals or alloys, e.g., aluminum and copper alloys, are needed to expand and attract interest in the usage of this joining technique, and this should result in its application in more industries. Friction stir welding was first used as a joining process and patented by The Welding Institute (TWI) of the UK in 1991 (TWI, United Kingdom). [5]. Friction stir welding works on the basic principle of friction generated between two parts due to relative motion between them. It is a solid-state joining technology in which a non-consumable tool with a specially designed pin and shoulder is inserted and rotated between the abutting edges of the plate to be joined. Then the tool is moved in a transverse direction when it touches the plates as shown in Figure 1.

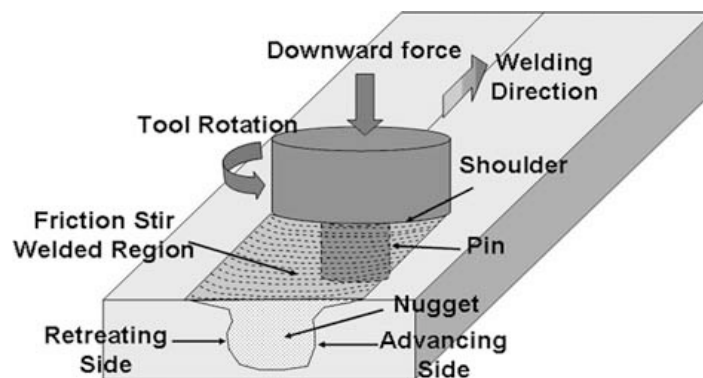


Fig. 1. Schematic view of Friction Stir Welding [6]

Concentrated heating of the plates softens the material at the tool and plates interface near the pin, and the dual motion of the tool, which is rotation and translation, results in the movement of material from the front to the back of the tool pin. Thus, a welded joint is obtained in solid state [6]. The tool geometry plays an important role in material flow and also governs the traverse rate of the process that can be conducted. This tool has two primary functions: (a) localized heating and (b) material flow [7]. It is an environmentally friendly technique involving energy efficiency and versatility to provide a satisfactory combination of microstructure and mechanical properties of the assemblies [8]. During the FSW process, the material undergoes intense plastic deformation at elevated temperature, which results in the generation of fine and equiaxed recrystallized grains [9], [10]. Due to the fine microstructure, friction stir welds produce good mechanical properties. FSW as shown in Figure 1 has been widely applied in the aerospace industry for the fabrication of high-strength aluminum alloy structures, such as some large-volume fuel tanks, due to its anomalous advantages over traditional fusion welding processes, including fewer defects, elevated mechanical properties, and low distortion of the joint. [11]

It has been reported that friction stir welding has advantages when compared with fusion welding processes. Problems, such as solidification cracking, porosity, and liquation cracking, are eliminated when using FSW due to its solid-state nature [12]. Furthermore, FSW provides numerous energy benefits, including the usage of only 2.5% of the energy needed for a laser weld and the reduction in fuel consumption in lightweight aircraft, automotive, and ship production [13].

### 1.1 Mechanical Properties of FSW Welded Joints

Mechanical properties play a vital role during the application of welded products. There has been vast research in which the mechanical properties of FSW joints have been investigated. The material characterization and the mechanical properties of the friction stir welded joints are influenced by several parameters. Tool geometry and process parameters like rotational speed, transverse speed, tool tilt angle, and downward force have been addressed by various researchers around the world.

El-Sayed et al. [14] investigated the impact of FSW variables on the peak temperature and the mechanical properties of AA5083-O welded joints. They concluded that the variation of both transverse speed and tool pin profile has a small effect on the welding peak temperature. Furthermore, they observed that utilizing a threaded tool pin at 50, 100, and 160 mm/min welding speeds produced defect-free welds with superior tensile strength values. Shah et al. [15] carried out FSW of AA6061 to assess the impact of tool eccentricity on the material flow and mechanical properties of the welded joints. Their consequences revealed superior material flow with tool offset as compared with the normal one, which resulted in expanding the soft region of the stir zone (SZ). However, the tool offset did not affect the mechanical properties of the welded joints. Rao et al. [16] displayed that increasing both the rotational and welding speed values leads to an improvement in the tensile properties. Moreover, a good mixing of the plasticized material and the best results were achieved by using the threaded tool pin profile. Azizi et al. [17] studied the impact of traverse speed change on the material characterization and the mechanical properties of thick pure copper welded joints. The results showed that finer grain sizes were achieved at elevated welding speed values due to minimal heat input and peak temperature, though defective joints were produced at these values. Moreover, raising the travel speed caused a rise in the tensile strength to an extreme value and was then followed by a reduction. It also indicated that raising the travel speed deeply affects the hardness, whereas it adversely influences the ductility; thereby, more ductile rupture was noticed at lower traverse speeds. Kalemba-rec et al. [18] scrutinized the impact of FSW variables on the mechanical properties of AA7075-T651 and AA5083-H111 dissimilar welded joints. They deduced that the joints' mechanical properties were adversely affected by the increase of rotational speed regardless of the shape of the tool pin profile. The efficiency of the joints by the Triflute tool pin profile reached 100% of the tensile strength value. Moreover, the pin geometry had a great widening impact on the shape of SZ, especially when using the Triflute pin profile. The breaking location of the defect-free welds was noticed at the softer material (i.e., AA5083). Sevel et al. [19] checked the microstructural evolution and the corrosion resistance of dissimilar AZ80A and AZ91C Mg welded joints. It was demonstrated that defect-free joints with excellent mechanical properties were achieved when AZ80A Mg alloy was located at the retreating side (RS) because of the easier material flow from the AS to the RS. In contrast, achieving defect-free joints was slightly difficult when this alloy was positioned at the AS. Sun et al. [20] examined dissimilar CuCrZr/CuNiCrSi joints microscopically and mechanically at various rotational speeds. The results displayed that raising the rotational speed caused an excess of both retreating material area and SZ grain size. The mechanical properties, such as micro-hardness and tensile strength, in the DXZ were adversely impacted by increasing the rotational speed.

Chaitanya Sharma et al. [21] investigated a high-strength Al–Zn–Mg alloy AA7039 at varying welding speeds and rotary speeds of the tool in order to predict the effect of varying welding parameters on microstructure and mechanical properties. This investigation predicted that the mechanical properties increased with decreasing welding speed/increasing rotary speed. This improvement may be due to increased heat input per unit length of the welded joint. The decrease in the welding speed and an increase in the tool rotary speed reduce the zigzag line formation

tendency. The minimum hardness region shifts to the weld nugget zone from the heat-affected zone on decreasing the tool rotary speed and increasing welding speed. The fracture of welded joints produced using high heat input occurred from HAZ (heat-affected zone) adjacent to the thermo-mechanically affected zone on the advancing side, while that of the joint developed using low heat input fractured from the weld nugget along the zigzag line on the advancing side.

### 1.2 Microstructure Evaluation of FSW Joints

Threadgill et al. [22] analyzed the microstructure evolution of friction stir welded aluminum joint and classified it into four zones as shown in Figure 2. This classification basically depends on the impact of both heat and plastic deformation created during welding. These zones are namely as follows:

- Base Material (BM): in which neither heating nor plastic deformation affects the material characterization.
- Heat-affected zone (HAZ): this zone is subjected to a thermal cycle without any plastic deformation, so the generated heat has no impact on the microstructure evolution.
- Thermo-mechanically affected zone (TMAZ): this zone is subjected to both heat and plastic deformation, which cause an effect on the microstructure characterization but without grain recrystallization due to insufficient deformation strain; however, dissolution of some precipitates may be observed as investigated by Mahoney et al. [23].
- Dynamically recrystallized zone (DXZ): it is also known as the “nugget zone.” In which, both high plastic deformation and high temperature cause dynamic recrystallization of grains. This region is characterized by an onion ring structure, which may be observed in the case of specific welding conditions.

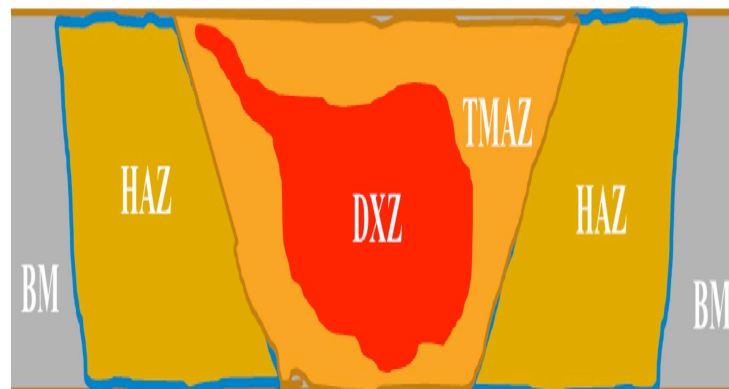


Fig. 2. Schematic representation of FS welded joint

Zhang et al. [24] assessed the influence of the shoulder-less FSW tool on the microstructure evolution and the mechanical properties of ultra-thin AA1060 welded joints. The results revealed that utilizing the shoulder-less tool caused a narrower weld area and lower attained heat, and hence a smaller HAZ is produced. As a result, the nugget zone hardness was higher than that of the BM, and the best achieved weld efficiency was 78.6% of the BM tensile strength. Pashazadeh et al. [25] performed the FSW process by using a non-threaded tool pin profile to investigate the effect of the shoulder plunge depth on the morphology and the microstructure of the copper alloy welded joints. The results reported the formation of four zones (surface layer, surface material, in-situ material, and TMAZ) in the RS of the SZ, and a surface layer was created by the shoulder-driven material. Furthermore, gradual variation in the grain size from the parent metal to the DXZ on the RS was observed, while a sudden change in the AS was reported. This was attributed to the diffused interface

in the former case and the sharpened look of the interface in the latter. Also, they showed that the weld was deeply affected by the materials on the retreating side. Nelson and Rose [26] investigated the impact of heat input and the backing plate material on the material characterization of HSLA steel welded joints. They deduced that the post-weld cooling rate had a great impact on the SZ microstructure over the range of welding conditions, where the hard zone in the HAZ disappeared at cooling rates below 20°C/S. Furthermore, they detected that raising the cooling rate from 7°C/S to 30°C/S, the lath width diminished linearly from 1.11  $\mu\text{m}$  to 0.59  $\mu\text{m}$ , and this caused an increase in the hardness values from 234 to 298 HV. They also noticed a proportional relation between the lath length and the heat input regardless of the backing plate material.

### 1.3 Tribological Aspects of FSW Welded joints

In the age of lightweight materials, aluminum alloys dominate the automobile and aircraft sectors. Aluminum alloys are used in durable, strong applications, but their poor wear resistance prevents their employment in cylinder blocks and brake shoes. They are limited in applications with substantial tribological difficulties. Thus, covering metallic substrates like aluminum alloys with ceramic powders extends component service life. Copper and its alloys are used in high-pressure vessels, condensers, and other power plants. Tribological examination of welded joints is understudied. FSW tribology must be studied for Al-Cu joints.

The pin-on-disk method was used to study the sample's wear behavior, and the results showed that treated samples have a lower friction coefficient than base metal. Also, AA 6061 aluminum alloy has lower wear resistance due to abrasion wear, while all other surface composites have higher wear resistance due to adhesive wear.

From the literature review it is observed that –

1. Some defects, including cracks, voids and pores are usually found in FSW.
2. When some process parameters are used, the presence of hard and brittle intermetallic compounds in those welds is detrimental; and it clearly affects the mechanical properties of the produced welds. Therefore, the optimization of process parameters and the usage of the right welding tool shapes is of importance when attempting to produce sound welds.
3. It was noticed that FSW between similar metals has been fairly research whereas the FSW of dissimilar metals and alloys is not yet well researched. Hence, more studies need to be undertaken to further understand, optimize the process and this could result in using the technology in various industries.
4. From the previous research it has been concluded that main focus of characterization of weld is only about mechanical properties like tensile strength, hardness, toughness and microstructure examination etc. But very only few researchers have conducted the tribological testing to know the behavior of weld under various frictional conditions. So the tribological aspects of FSW need to be investigated for dissimilar metals.

To the best of the authors' knowledge, no previous study has reported a functionally graded citrus peel powder reinforced epoxy composite with layer-wise reinforcement distribution for simultaneous enhancement of mechanical performance and environmental durability

Mechanical and tribological properties play a vital role in developing any product for making it useful for its industrial application. The optimum tribological properties can be obtained by using the correct input parameters. So the main objectives of this research work are –

1. Fabrication of welded joints of dissimilar metals using Friction Stir welding.
2. Tribological characterization of welded joints.

3. Analysis of experimental data and finding of correct parameters for optimum tribological properties.

And to achieve the objectives of this research work, following methodology is suggested-

1. Selection of material to conduct Experimentation.
2. Selection of tool material based on previous research.
3. Conduction of the pilot experimentation on FSW setup.
4. Fabrication of FSW joints of dissimilar joints
5. Tribological characterization of welded specimen.
6. Microstructure analysis
7. Analysis of experimentation results.

### 3. Materials and Methods

#### 3.1 Materials

Sheets of pure copper C11000 and pure aluminum Al1060 were chosen. In this present investigation, sheets of 3 mm thickness were used. Specimen edges were properly milled and degreased before welding for attaining a proper weld joint.

#### 3.2 Machine and tool

The friction stir welding machine used for welding could monitor force and torque. Standardized methods are being used for clamping and backing plates which leads to the decreased heat loss and movement. Figure 3 shows the pictorial view of FSW machine with fixtures.

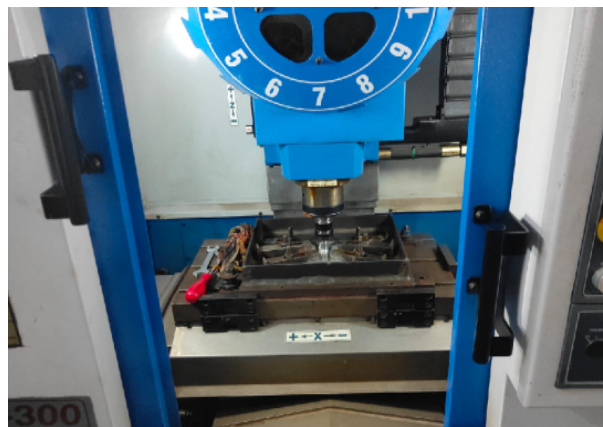


**Fig. 3.** FSW machine with fixtures

D2 tool steel as shown in Figure 4 was used to make the friction stir welding tool and it was tempered and hardened according to the as per the demand of the raw materials to be welded. The tool shoulder diameters tested were 18, 20 and 22 mm; pin profile was a threaded cylindrical/conical pin with nominal pin length matching plate thickness minus 0.1–0.2 mm.

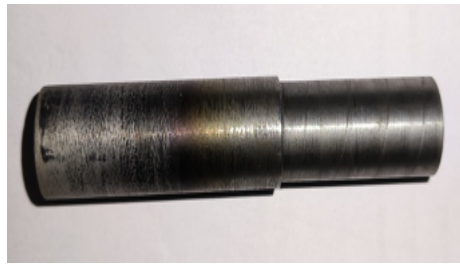


**Fig. 4.** D2 Steel Tool

### 3.3 Experimental Design

An L9 orthogonal array of Taguchi Analysis was selected for three factors with three levels each. The three most representative factors selected are: the diameter of the device shoulder, the rotating speed of the tool, and the travel welding speed. The different levels for these three factors are 18 mm, 20 mm, and 22 mm; 800 rpm, 1000 rpm, and 1200 rpm; and 90 mm/min, 120 mm/min, and 150 mm/min, respectively. The selection of these levels is based on previous research and preliminary trials. The systematic combinations of these factors in an L9 orthogonal array allow the overall quantity of experimental runs to be limited, and simultaneously, they preserve the statistical significance of the data. Table 1 shows the different selected parameters and their corresponding levels.

**Table 1**

Factors with their corresponding levels for FSW

Factors ↓ Levels →	1	2	3
Shoulder diameter (mm)	18	20	22
Tool rotational speed (rpm)	800	1000	1200
Welding speed (mm/min)	90	120	150

After inserting the input data into Minitab19 software L<sub>9</sub> orthogonal array as shown in table 2 has been found most suitable for Taguchi analysis.

**Table 2**

L<sub>9</sub> Orthogonal Array

Run	Shoulder (mm)	Rotational Speed (rpm)	Welding Speed (mm/min)
1	18	800	90
2	18	1000	120
3	18	1200	150
4	20	800	120
5	20	1000	150
6	20	1200	90
7	22	800	150
8	22	1000	90
9	22	1200	120

### 3.4 Sample preparation and mechanical testing

The Friction stir welding starts with firmly clamping the aluminum and copper sheets. Proper clamping is necessary to prevent any movement during the welding process. Then the non-consumable rotating D2 steel tool with a shoulder and a pin is positioned above the joint line between the two sheets. Then this rotating tool is pressed into the joints of the two sheets. Friction between

this tool and the joint of two sheets generates localized heat, which softens the material in the vicinity of the pin without melting it. After inserting the tool to the required depth, it is held there for a small period of time. By doing so, the material at the joint is heated and plasticized, making it sufficiently soft for stirring. The tool will follow the joint line during its forward motion, and at the same time, the pin stirs and mixes the softened material on both sides, while the shoulder forges the material behind the tool and adds more frictional heating, leading to a solid-state bond. Material from both the advancing and retreating sides flows around the pin as a result of the tool's rotation, mixing and solidifying in its wake, due to which the weld zone develops a fine-grained microstructure. A fine-grained microstructure forms in the weld zone as a result of material from the retreating and advancing sides flowing around the pin from the tool's rotation, mixing and solidifying in its wake. The tool is gradually withdrawn when it reaches at the end of the weld joint and completes the welding. The Figure 5 shows the initial, middle, and final stage of first specimen fabricated using FSW.

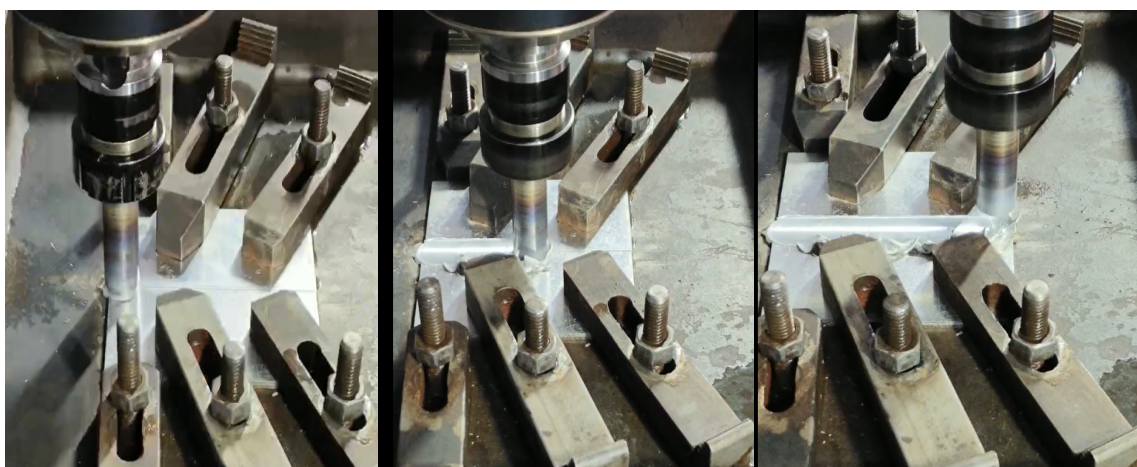


**Fig. 5.** Three images showing initial, middle and final welding process stages

The FSW Al–Cu joint is ready for a pin-on-disc wear test to study the tribological properties of this material system (i.e., friction coefficient and wear resistance) at the weld interface. Specimens are machined from the FSW plate with the weld line at the diametric location of the test disc to be tested. This procedure guarantees that the pin slides from the aluminum zone to the copper one through the weld nugget and enables testing friction and wear in all three zones. The specimens are turned to cylinders with a diameter of 40 mm and a thickness of 4–6 mm, and then water-cooled cutting is applied in order to avoid changes in the weld microstructure. Both surfaces are precision ground and then polished by SiC abrasive papers with increasing grit ranging from 320 to 1200.

Each disk rotates at a constant speed (0.1–1.0 m/s); friction between the pin and specimen generates wear conditions through heat generation and material transfer, while friction force and wear behavior are evaluated according to established pin-on-disc tribological testing procedures and wear analysis methods [26, 27]. The friction force is continuously monitored by a calibrated load cell, and the data acquisition software records simultaneously normal and tangential forces in order to determine the coefficient of friction. The obtained data (coefficient of friction vs. time, specific wear rate) are used to relate the FSW microstructure, in particular the outcome of a fine-grained weld nugget as well as intermetallic layers, with its tribological behavior. Figure 6 shows an Aluminum–Copper Specimen ready for Pin-on-Disc Wear Test.

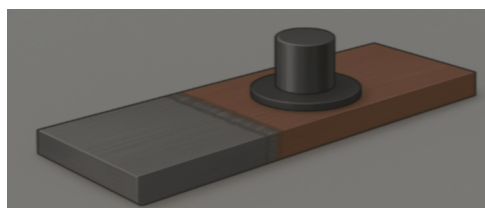


Fig. 6. Aluminum–Copper Specimen for Pin-on-Disc Test

The tests have been performed on all the nine samples and the values of wear rate ( $\text{mm}^3/(\text{Nm})$ ) and friction force (N) has been observed and noted as shown in Table 3.

**Table 3**

Experimental results of friction force and wear rate

Run	Shoulder (mm)	Rotational Speed (rpm)	Friction Force (N)	Wear rate ( $\text{mm}^3/\text{Nm}$ )
1	18	800	1600	0.009
2	18	1000	1350	0.0075
3	18	1200	1400	0.006
4	20	800	1500	0.008
5	20	1000	1250	0.0087
6	20	1200	1100	0.0055
7	22	800	1200	0.01
8	22	1000	1400	0.0078
9	22	1200	1000	0.0045

### 3.5 Microstructural analysis

Microstructural characterization of the weld in a friction stir welded (FSW) joint is very important to comprehend the integrity and performance of a FSW joint. SEM provides a clear distinction of separate weld zones. It offers high-quality imaging capabilities used for weld defects including void, tunnels, and cracks and on dissimilar joints. In addition, SEM examination of worn surfaces provides information delamination and groove formation. The weld cross sections were mounted, ground and polished and etched for clear images using optical microscopy.

## 4. Results

### 4.1 Taguchi analysis

#### 4.1.1 Taguchi Analysis for Friction Force

However, the resistance between the tool and the workpiece during friction stir welding is reduced by applying the principle of "small is better." According to the S/N ratio as shown in Table 4, RPM showed the highest delta value (1.81), which means that it was the most influential among all studied levels in friction force, followed by shoulder diameter (1.70) and welding speed (0.57). This order of preference ( $\text{RPM} > \text{SH} > \text{WS}$ ) reveals that the friction character is mainly controlled by the rotational velocity of the tool, which regulates heat generation and material softening at the interface. With higher RPM, more rotating motion contributes to frictional heating and plastic deformation, which may cause larger friction force. In contrast, at lower to moderate RPMs, the tool feels or senses a more gentle material flow with less resistance and hence has a reduced friction force. The effect of shoulder diameter is also significant, and the larger shoulders yield a higher contact area and more severe friction, while the welding speed plays less in comparison. Therefore, the rotation speed is a very important process parameter in that it directly influences the homogeneous flow of material, uniform input of heat, and minimal friction during processing. Table

4 shows the S/N Ratios (Smaller is better) and Figure 7 shows the main effects plot for S/N ratio for friction force.

**Table 4**

Response Table for S/N Ratios (Smaller is better) for Friction Force

Level	Shoulder (mm)	RPM	Weld Speed (mm/min)
1	-63.20	-63.06	-62.61
2	-62.10	-62.49	-62.04
3	-61.50	-61.25	-62.15
<b>Delta</b>	1.70	1.81	0.57
<b>Rank</b>	2	1	3

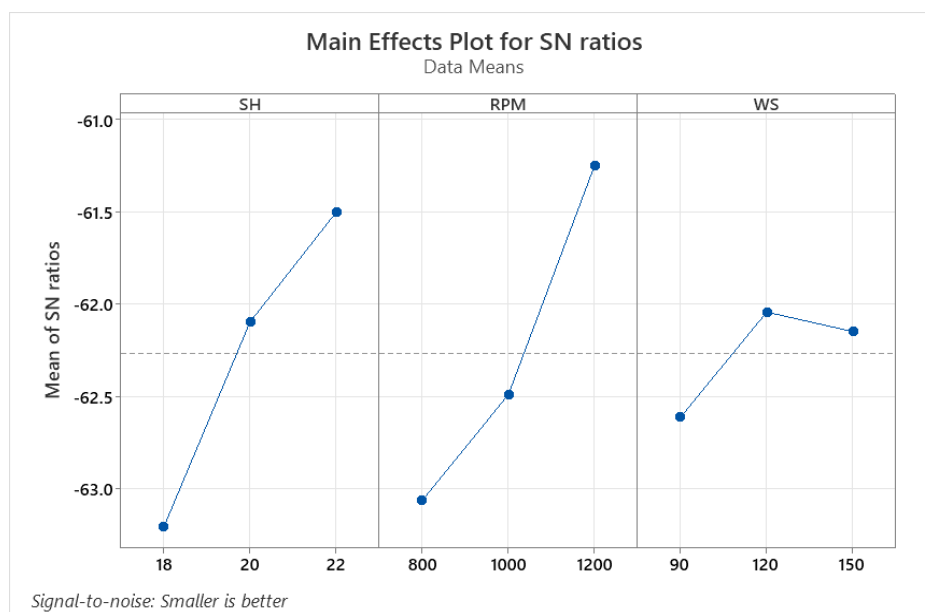


**Fig. 7.** Main effects plot for S/N ratio for friction force

#### 4.1.1 Taguchi Analysis for Wear Rate

The Taguchi approach to Wear Rate has also been used with the criterion that "smaller is better" for reducing material loss during weld deposition. Based on the S/N ratio response as shown in Table 5, rotational speed (RPM) showed the highest delta value (4.57) and was also the most influential factor, followed by welding speed (1.91) and shoulder diameter (0.41). The order of this hierarchy (RPM > WS > SH) indicates that tool wear is strongly influenced by rotational speed, as it significantly affects the production level of frictional heat and time of tool-workpiece contact. The surface temperature and frictional stress are increased at a higher rotation speed, resulting in accelerated tool wear by severe abrasion and adhesion. However, too low RPM can have the effect of insufficient softening, with the result that facade/tool mechanical overloading occurs. As a result, when the speed of rotation is at this moderate level, there will be appropriate plasticization and limited wear. Weld speed affects the wear as well: too high of a speed may inhibit mixing and increase stress on the tool, but a slower speed can accelerate material flow, though this has subsequently prolonged contact. The SHD has the lowest influence because it is less important in heat generation. Thus, tool wear and process efficiency can both be reduced by optimizing an appropriate synthesis of moderate RPM, balanced welding speed, and proper shoulder size. Table 5 shows the S/N Ratios (Smaller is better) and Figure 8 shows the main effects plot for S/N ratio for wear rate.

**Table 5**  
 Response Table for S/N Ratios (Smaller is better) for Friction Force

Level	Shoulder (mm)	RPM	Weld Speed (mm/min)
1	42.62	40.95	42.76
2	42.78	41.96	43.79
3	43.03	45.52	41.88
<b>Delta</b>	0.41	4.57	1.91
<b>Rank</b>	3	1	2

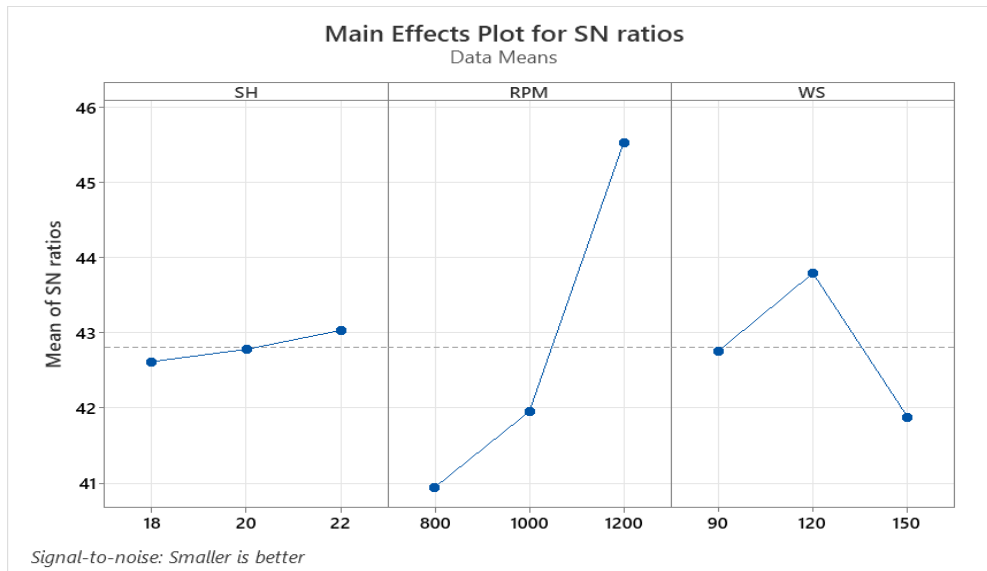


**Fig. 8.** Main effects plot for S/N ratio for wear rate

## 4.2 ANOVA analysis

### 4.2.1 ANOVA for friction force

Table 6 shows the calculations of different parameters necessary for making an accurate ANOVA for friction force.

**Table 6**  
 ANOVA analysis for Friction Force (S/N ratio)

Source	SS	DF	MS	F	% contribution
<b>RPM</b>	108,888.89	2	54,444.44	1.474	37.05%
<b>Shoulder (SH)</b>	97,222.22	2	48,611.11	1.316	33.08%
<b>Weld Speed (WS)</b>	13,888.89	2	6,944.44	0.188	4.73%
<b>Error</b>	73,888.89	2	36,944.44	—	25.14%

The ANOVA of friction force showed that temperature as rotational speed (RPM) has a major role in the control of the friction resistance during FSW, accounting for  $\approx 37\%$  in the global variance. Shoulder diameter made a contribution of  $\approx 33\%$ , and the welding speed was relatively insensitive ( $\approx 5\%$ ). They were not significantly different at the 95% confidence level because of the low residual degrees of freedom in the  $L_9$  orthogonal array (single-replicate design), but practical trends can be observed and considered. The friction force dramatically reduced with increasing rotational frequency and achieved the lowest values at approximately 1200 RPM, which indicated better material softening and a more favorable plastic flow. Also, larger diameters of shoulders tended to decrease the friction by the more uniform generation of heat. Therefore, albeit the significance is

not strong enough, ANOVA results obviously reflect that imposing a higher RPM and a larger shoulder diameter result in a reduction of friction force in FSW.

#### 4.2.2 ANOVA for friction force

Table 7 shows the calculations of different parameters necessary for making an accurate ANOVA for wear rate.

**Table 7**  
 ANOVA analysis for Wear Rate (S/N ratio)

Source	SS	DF	MS	F	% contribution
RPM	0.00002155556	2	0.000010	86.607	84.52%
Shoulder (SH)	0.00000368222	2	0.0000018	14.795	14.44%
Weld Speed (WS)	0.00000001556	2	0.000000	0.0625	0.06%
Error	0.00000024889	2	0.0000001	—	0.98%

The ANOVA analysis for the wear rate showed a stronger trend and was more statistically significant, with the factor of rotational speed being the most powerful source of variation (with a contribution to total variation of  $\approx 84.5\%$ ), and it was found RPM exhibited the highest contribution ratio (84.52%) and the largest F-value (86.61), indicating its dominant influence on wear rate. The effect of welding speed was moderate with  $\approx 14.4\%$  contribution; however, the Shoulder diameter contributed 14.44% of the total variation. The wear rate continuously reduced with the increase in rotation speed till 1200 RPM; therefore, it can be concluded that high penetration heat input and stable material softening reduce abrasive and adhesive wear of the tool. The welding speed showed a similar trend and presented the lowest wear at 120 mm/min among the considered levels, indicating that both extremely fast and slow welding speeds can elevate tool-workpiece strain. In summary, the ANOVA results unambiguously indicate that RPM is the most significant (i.e., controlling) control factor for wear reduction, with weld speed as a secondary (significant in practice but second-order) effect; it can be ‘fine-tuned’ to tailor wear performance during FSW.

The synergy of the results of Taguchi, GRA, and ANOVA has well explained the effect of FSW parameters on friction force and wear rate in great detail. Among all the statistical techniques, rotational speed (RPM) was found to be a highly influential factor affecting the tribological behavior of the process. Taguchi S/N ratio analysis indicated the higher delta values of RPM for friction force and wear rate, indicating that RPM is highly influenced by the friction effect, heat generation, and material softening. This tendency was further confirmed by GRA, where Run 9 (SH = 22 mm, RPM = 1200, WS = 120 mm/min) was identified as the best combination of parameters, which gives the lowest value of friction force and wear rate at the same time. This optimal run presents the best balances of thermal-mechanical conditions as sufficient heat is input and flows into the polymer to decrease resistance while minimizing material degradation.

The ANOVA results provided further statistical confirmation of these effects. As for the friction force, RPM contributed 37% of the total variation, closely followed by shoulder diameter at about 33%, which means that these two set points have a significant effect on sealing behavior during friction welding. The impact of the factors was not significant at the 95% confidence level because of the small degrees of freedom in the  $L_9$  design, but the physical influence and trends were still vivid and consistent with process behavior. In contrast, ANOVA of wear rate presented a strongly significant trend, and RPM was responsible for  $\approx 84.5\%$  of variation with a very statistical F-value.

Welding speed made a moderate ( $\approx 14\%$ ) contribution, and shoulder diameter had an insignificant influence on tool wear. These results confirm the tool wear to be significantly influenced by the thermal and mechanical conditions prescribed by speed, as insufficient or excessive heat leads directly to abrasive or adhesive abrasion mechanisms.

#### 4.3 Grey Relation Analyses

The GRA was used to obtain the best possible combination of parameters that minimizes wear rate and friction force at the same time. The normalized size was determined by the “the smaller the better” principle, deviation sequences, and GRC calculation. Finally, the average value of Grey Relational Grade (GRG) was calculated with respect to each experimental run for multi-response performance coating. Table 8 shows the values calculated during different steps of Grey Relation analysis for the two responses.

**Table 8**

Normalization, Deviation, GRC and GRG for each run (higher GRG = better)

Run	Normalized Values (Friction)	Normalized values (Wear)	Devi. Seq. (Friction)	Devi. Seq. (Wear)	GRC Friction	GRC Wear	GRG
1	0.181818182	0	0.818182	1	0.37931	0.33333	0.3563
2	0.454545455	0.416666667	0.545455	0.5833333	0.47826	0.46153	0.4698
3	0.727272727	0.333333333	0.272727	0.6666666	0.64705	0.42857	0.5378
4	0.363636364	0.166666667	0.636364	0.8333333	0.44	0.375	0.4075
5	0.236363636	0.583333333	0.763636	0.4166666	0.39568	0.54545	0.4705
6	0.818181818	0.833333333	0.181818	0.1666666	0.73333	0.75	0.7416
7	0	0.666666667	1	0.3333333	0.33333	0.6	0.4666
8	0.4	0.333333333	0.6	0.6666666	0.45454	0.42857	0.4415
9	1	1	0	0	1	1	1

From Table 8, it is clear that Run 9 has the highest GRG value (GRG=1.000; RANK 1), followed by Run 6 (GRG=0.7417; RANK 2) and then followed by Efficiency Run 3 (GRG=0.5378; RANK 4). These runs are the best combination of process parameters for optimum wear and friction force simultaneously. The lowest GRG value (0.3563, Run 1) indicates the least efficient combination. This order indicates that the parameter condition of Run 9 results in the best performance overall, representing suitable trade-offs between heat generation, material flow, and tool-workpiece contact.

In general, from the ball-on-disk wear results obtained from GRA, it is evident that optimizing process parameters such as appropriate rotational speed and a controlled shoulder diameter could significantly improve both tribological responses. Thus, Run 9 is identified as the best parameter combination, which produces a good trade-off between low wear and low friction force to extend tool life for better weldment’s characteristics and process performance.

Collectively, combining the results of Taguchi, GRA, and ANOVA, it is found that RPM is more influential than welding speed and shoulder diameter for optimization of FSW performance. The optimum combination found by GRA (Run 9) exhibits a remarkable decrease in both the friction force and wear rate, thus resulting in improved tool life, better material flow, and better weld quality. These consistent results from a variety of analytical tools confirm the stability of the parameter trends identified and offer a robust platform with which to optimize process conditions to achieve both efficient processing and superior tribological performance during friction stir welding.

#### 4.4 SEM Analysis of worn surface

Figure 9 (a) shows SEM pictures of the worn surface of a sample after a wear test using the pin-on-disc approach. It depicts the wear holistic morphology formed under pin-on-disc test conditions for an Al–Cu alloy surface. The surface presents large, continuous grooves oriented in the direction of the indicated sliding, indicating that abrasive ploughing was the predominant wear process at this scale. These scratches are caused by sharp, hard SiC particles in the abrasive sheet impinging into and ploughing the surface during sliding. In addition to ploughing marks, the existence of a partly detached surface layer and micro-cracks indicates the initiation of delamination wear due to repetitive subsurface shear stresses and material failure. The development of linear abrasive grooves in conjunction with premature delamination was indicative of mixed abrasive and fatigue wear experienced by the Al–Cu alloy sliding against the CWS under the selected test conditions.

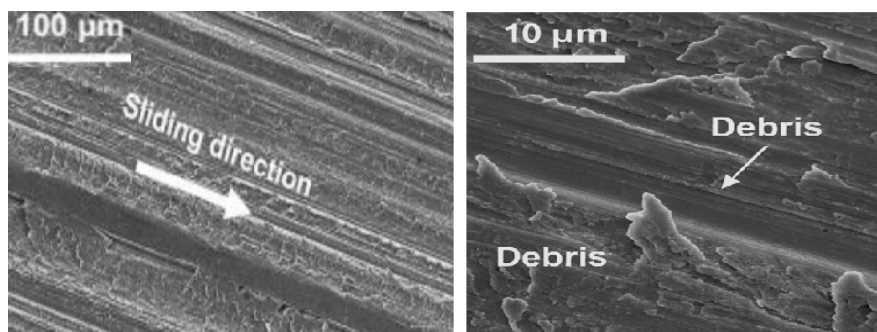


**Fig. 9 (a,b)** SEM images of Worn surface

Figure 9 (b) shows a higher magnification of the worn surface and agglomeration of debris with delamination flakes is observed along the wear groove edges. The debris is not well-packed, and its shape is irregular, and the distribution of it along the groove boundaries indicates that pieces were released from the surface during sliding as subsurface cracks propagated towards/through the top layer. At this resolution, the valleys look much deeper and more distinct. The fragmented lamellar debris illustrated here is a typical feature of severe delamination wear, in which the layers come off after exhaustion through cyclic plastic deformation. This detailed morphology reveals that the Al–Cu alloy at micro-scale is subjected to heavy abrasive cutting and then progressive delamination to form rough, debris-filled wear tracks.

#### 5. Conclusion

The present study investigated the effect of rotational speed, shoulder diameter, and welding speed on the friction force and wear rate during friction stir welding using the Taguchi method, Grey Relation Analysis (GRA), and ANOVA. The combined results identified rotational speed as the most influential parameter affecting both responses. Higher rotational speed resulted in lower friction resistance and wear due to improved heat generation and stable material flow. According to the Taguchi and GRA results, the optimum process parameters combination was found to be a shoulder diameter of 22 mm, rotational speed of 1200 RPM and welding speed of 120 mm per minute for simultaneous minimization of friction force and wear rate. Under these conditions, the minimum friction force and wear rate achieved were 1000 Newton and 0.0045 mm<sup>3</sup>/Nm respectively. These values represent the best tribological performance among all the Experimental runs conducted in the present study.

These findings are corroborated by ANOVA results that reveal the dependence of both responses on rotational speed, with a significant effect on wear rate. The influence of welding speed is moderate, and shoulder diameter is less pronounced. In general, integration of Taguchi-GRA with ANOVA provides a successful and reliable solution for the multi-response optimization in FSW. The optimum process parameters obtained will lead to improved tribological behavior, ease of material flow, and tool wear during FSW, resulting in increased efficiency. SEM analysis showed that abrasive and delamination wear occurs by pin-on-disc test during the Al–Cu alloy. Microstructural investigation is used to detect gradual subsurface cracking and material removal arising from the loading conditions and sliding contact. These findings establish a dependable foundation for the selection of proper process parameters in the subsequent Friction Stir welding practice.

The current study is within a range of parameters for friction stir welding (shoulder diameters from 18 to 22 mm, rotational speeds from 800 to 1200 rpm, and welding speeds from 90 to 150 mm/min). Only D2 tool steel was used, so the influence of different tooling materials was not investigated. In addition, the tribological characterization is performed only in a unique load, sliding speed, and temperature, and service environments were not performed. Future studies should explore a broader parameter space, different tool materials, and more diverse tribological loading conditions to provide greater transferability for the results.

### Acknowledgement

This research is not funded by any institute or agency. Also we are thankful to Dr. Anil Kumar, Assistant Professor, DSEU, New Delhi for his assistance in computational work.

### Reference

- [1] Kumar, V., and S. Kumar. "A Review Report on Mechanical Properties of Al 6106 T6 Alloy Joined by Friction Stir Welding and TIG Welding." *International Journal of Applied Science Technology Research Excellence* 6, no. 2 (2016).
- [2] Hartley, P. J., D. E. Hartley, and A. McCool. "Implementation of Friction Stir Welding on the Space Shuttle External Tank." In *Proceedings of the 3rd International Symposium on Friction Stir Welding*. Kobe, Japan, 2002.
- [3] Kallee, S. W. "Application of Friction Stir Welding in the Shipbuilding Industry." In *Lightweight Construction for Shipbuilding Applications*, 25–35. London: Royal Institution of Naval Architects, 2000.
- [4] Smith, C. B., J. F. Hinrichs, and W. A. Crusan. "Robotic Friction Stir Welding: The State of the Art." In *Proceedings of the Fourth International Symposium on Friction Stir Welding*, 14–16. 2003.
- [5] Thomas, W. M., E. D. Nicholas, J. C. Needham, M. G. Murch, P. Templesmith, and C. J. Dawes. "Friction Stir Welding." Patent Application No. 9125978.8, 1991.
- [6] Ma, Z. Y. "Friction Stir Processing Technology: A Review." *Metallurgical and Materials Transactions A* 39 (2008): 642–658. <https://doi.org/10.1007/s11661-008-9470-0>.
- [7] Mishra, R. S., and Z. Y. Ma. "Friction Stir Welding and Processing." *Materials Science and Engineering R* 50 (2005): 1–78. <https://doi.org/10.1016/j.mser.2005.07.001>.
- [8] Chen, Y. C., and K. Nakata. "Effect of Surface State of Steel on Microstructure and Mechanical Properties of Dissimilar Lap Joints by Friction Stir Welding." *Metallurgical and Materials Transactions A* 39A (2008): 1985–1992. <https://doi.org/10.1007/s11661-008-9571-9>.

- [9] Rhodes, C. G., M. W. Mahoney, W. H. Bingel, R. A. Spurling, and C. C. Bampton. "Effects of Friction Stir Welding on Microstructure of 7075 Aluminium." *Scripta Materialia* 36, no. 1 (1997): 69–75. [https://doi.org/10.1016/S1359-6462\(96\)00302-5](https://doi.org/10.1016/S1359-6462(96)00302-5).
- [10] Benavides, S., Y. Li, L. E. Murr, D. Brown, and J. C. McClure. "Low-Temperature Friction Stir Welding of 2024 Aluminum." *Scripta Materialia* 41 (1999): 809–815. [https://doi.org/10.1016/S1359-6462\(99\)00221-7](https://doi.org/10.1016/S1359-6462(99)00221-7).
- [11] Wang, G., Y. Zhao, and Y. Hao. "Friction Stir Welding of High-Strength Aerospace Aluminum Alloy and Application in Rocket Tank Manufacturing." *Journal of Materials Science and Technology* 34, no. 1 (2018): 73–91. <https://doi.org/10.1016/j.jmst.2017.10.015>.
- [12] Lienert, T. J., W. L. Stellwag Jr., B. B. Grimmer, and R. W. Warke. "Friction Stir Welding Studies on Mild Steel." *Welding Journal* 82, no. 1 (2003): 1s–9s.
- [13] Mishra, R. S., and M. W. Mahoney. "Introduction." In *Friction Stir Welding and Processing*. Materials Park, OH: ASM International, 2007.
- [14] El-Sayed, M. M., A. Y. Shash, T. S. Mahmoud, and M. Abd-Rabbou. "Effect of FSW Parameters on Peak Temperature and Mechanical Properties of Aluminum Alloy 5083-O." *Advanced Structured Materials* 72 (2018): 11–25. [https://doi.org/10.1007/978-3-319-76276-7\\_2](https://doi.org/10.1007/978-3-319-76276-7_2).
- [15] Shah, L. H., S. Guo, S. Walbridge, and A. P. Gerlich. "Effect of Tool Eccentricity on Properties of Friction Stir Welded AA6061." *Manufacturing Letters* 15 (2017): 14–17. <https://doi.org/10.1016/j.mfglet.2017.07.002>.
- [16] Rao, A. N., L. S. Naik, and C. Srinivas. "Evaluation of Tool Profile and Rotational Speed on Friction Stir Welded Copper Alloy 2200." *Materials Today: Proceedings* 4, no. 2 (2017): 1225–1229. <https://doi.org/10.1016/j.matpr.2017.01.139>.
- [17] Azizi, A., R. V. Barenji, A. V. Barenji, and M. Hashemipour. "Microstructure and Mechanical Properties of Friction Stir Welded Thick Copper Plates." *International Journal of Advanced Manufacturing Technology* 86 (2016): 1985–1995. <https://doi.org/10.1007/s00170-015-8199-3>.
- [18] Kalembe-Rec, I., M. Kopy, D. Miara, and K. Krasnowski. "Effect of Process Parameters on Mechanical Properties of Dissimilar Friction Stir Welded 7075-T651/5083-H111 Alloys." *International Journal of Advanced Manufacturing Technology* 97 (2018): 2767–2779. <https://doi.org/10.1007/s00170-018-2044-z>.
- [19] Sevel, P., and V. Jaiganesh. "Influence of Material Arrangement and Microstructural Analysis during FSW of AZ80A and AZ91C Mg Alloys." *Archives of Metallurgy and Materials* 62 (2017): 1795–1801. <https://doi.org/10.1515/amm-2017-0265>.
- [20] Sun, Y., D. He, F. Xue, and R. Lai. "Effect of Tool Rotational Speed on Microstructure and Mechanical Properties of CuCrZr/CuNiCrSi Butt Joint." *Metals* 8 (2018): 526. <https://doi.org/10.3390/met8070526>.
- [21] Sharma, C., D. K. Dwivedi, and P. Kumar. "Effect of Welding Parameters on Microstructure and Mechanical Properties of Friction Stir Welded AA7039." *Materials and Design* 36 (2012): 379–390. <https://doi.org/10.1016/j.matdes.2011.11.034>.
- [22] Threadgill, P. L., A. J. Leonard, H. R. Shercliff, and P. J. Withers. "Friction Stir Welding of Aluminium Alloys." *International Materials Reviews* 54, no. 2 (2009): 49–93. <https://doi.org/10.1179/174328009X411136>.
- [23] Mishra, R. S., M. W. Mahoney, S. X. McFadden, N. A. Mara, and A. K. Mukherjee. "High Strain-Rate Superplasticity in Friction Stir Processed 7075 Al Alloy." *Scripta Materialia* 42 (2000): 163–168. [https://doi.org/10.1016/S1359-6462\(99\)00400-X](https://doi.org/10.1016/S1359-6462(99)00400-X).

- [24] Zhang, C., W. Wang, X. Jin, C. Rong, and Z. Qin. "Micro Friction Stir Welding of Ultra-Thin Al-1060 Sheets Using Shoulderless Tool." *Metals* 9 (2019): 507. <https://doi.org/10.3390/met9050507>.
- [25] Pashazadeh, H., J. Teimournezhad, and A. Masoumi. "Material Flow and Mechanical Properties in Friction Stir Welding of Copper Sheets." *International Journal of Advanced Manufacturing Technology* 88 (2016): 1961–1970. <https://doi.org/10.1007/s00170-016-8924-8>.
- [26] ASTM G99-17. *Standard Test Method for Wear Testing with a Pin-on-Disk Apparatus*. West Conshohocken, PA: ASTM International, 2017. <https://doi.org/10.1520/G0099-17>.
- [27] Stachowiak, G. W., and A. W. Batchelor. *Engineering Tribology*. 4th ed. Oxford: Butterworth-Heinemann, 2014.